Numerical Study of Bio-Inspired Corrugated Airfoil Geometry in a Forward Flight at a Low Reynolds Number

YAGYA DUTTA DWIVEDI[1], SUDHIR SASTRY Y. B.[2], BDY SUNIL[1],
CH. V. K. N. S. N. MOORTHY[3], K. VISWANATH ALLAMRAJU[1]
[1]Department of Aeronautical Engineering, Institute of Aeronautical Engineering, Dundigal, Hyderabad, Telangana, 500043, INDIA
[2]Department of Aerospace Engineering, International Institute of Aerospace Engineering and Management, Jain Deemed to be
University, Bengaluru, 562112, INDIA
[3]Vasavi College of Engineering, Ibrahimbagh, Hyderabad, Telangana, 500031, INDIA

Abstract: - In this study, the effects of variations in the parametric geometry on the aerodynamic efficiency and longitudinal static stability of a bio-inspired airfoil were assessed using the computational method at a low Reynolds number of 80000. The investigation aims to recognize the influence of corrugations on aerodynamic forces and moments and compare them with a non-corrugated profile having similar geometry without corrugations. Three different airfoils were chosen, the first triangular peaked corrugated is inspired from the mid-section of a dragonfly wing, the second modified simplified corrugated is a different form of the dragonfly wing section, which was modified to match the maximum thickness of the first airfoil, and the third is a non-corrugated Hybrid airfoil obtained by joining the peaks of the second airfoil. These three models were fabricated using an additive manufacturing process to undertake the experimental work in a low subsonic wind tunnel to find aerodynamic characteristics. ANSYS FLUENT solver was applied to unravel the steady, laminar, incompressible, two-dimensional, RANS equations. The tests were performed for 4 to +20 degrees angle of attack at a Reynolds number of 80,000. The result revealed that the Hybrid airfoil is suitable only for up to a 4-degree angle of attack. The modified simple corrugated airfoil produced significant aerodynamic performance at high angles of attack than the other two tested airfoils. The flow field study also showed the same results. Results are validated with experimental work and also with existing literature.

Key-Words: Aerodynamic performance, static stability, Bio-inspired corrugated airfoil, low Reynolds number, computational fluid dynamics

Received: May 29, 2021. Revised: April 18, 2022. Accepted: May 15, 2022. Published: July 12, 2022.

1 Introduction

Over millions of years, Nature has evolved all avians and insects to have definite wings. By flapping, avians can create sufficient lift and thrust force to make them highly maneuverable, fly easily, and sustained endurance. Due to these qualities, researchers have taken a lot of interest to understand the said field of the flapping wing over the past few decades. Consequently, this has given me the advantage to understand deeper flapping wing aerodynamics, which paves the way for the better design of future micro aerial vehicles (MAVs).

Biologists discovered that the dragonfly is one of the most agile insects of nature, which fly at a low-Re regime [1], [2] during the 1970s and 1990s. The dragonfly (Aeshna cyanea) forewing mid- cross-section is characterized by well-defined corrugations with varying dimensions over the span from root to tip. The corrugated wing of the dragonfly demonstrates sufficient hovering capability [3] and also enhances considerably bending resistance during flapping [4]. Further study revealed that there is a considerable enhancement of aerodynamic performance (high L/D) due to corrugations [5] or having insignificant sensitivity of the Re variations[6]. Later some experimental analyses showed that the corrugated airfoil outclassed the conventional airfoil operating in low-Re conditions [7], [8].These studies have generated interest in the researchers to try and to understand the causes for the enhancement of the aerodynamic performance and stability of corrugated wings inspired by the dragonfly. Some numerical work was performed and showed trapped unsteady vortexes inside the valleys of the corrugation[9]. These unsteady vortexes produce low pressure on the upper surface and enhance lift force and promote the transition from laminar to turbulent boundary layers flow and attach to the upper surface. The turbulent flow owns higher kinetic energy than laminar flow so it will overcome the negative pressure gradient. This phenomenon reduces the flow separation and delays the stall of the airfoil [8].Another important numerical study [10] has demonstrated that there exists a strong negative pressure between the leading edge (LE) and the first corrugation. The next corrugations also generate depression with lesser intensity than the first corrugation. The most severe suction zone that exists between the LE and the first corrugation, is the principal cause of the enhanced lift and reduced drag. Seifert and Levy [11], have undertaken a study to explain the behavior of the flow around multiple models of corrugated airfoils. They explained that the flow accelerates around the leading edge, and boundary layers appear to be detached, which is reattaching the backward part of the airfoil and reducing flow separation.

Even though most of the above studies have focused to understand the flow pattern and aerodynamic efficiency of bio-inspired corrugated airfoils and most of them have compared results with a flat plate. The flat plate does not have any camber and also maximum thickness of the flat plate cannot be compared with the bio-inspired corrugated airfoil.Therefore, the comparison with flat plate and the knowledge gained in previous work, can't be used for comprehension of the effects of corrugations in the current state. In the present work, the bio-inspired airfoil taken from the dragonfly mid-span is obtained from the work of Tamai and Hu [8]. This airfoil is then filled with material, so the corrugations are removed and the geometrical parameters are identical to the bio-inspired airfoil called hybrid airfoil and then compared the aerodynamic characteristics computationally. Another airfoil which is also bio-inspired corrugated has identical geometry except the maximum thickness location is shifted towards the trailing edge by 0.1c from the previous bio-inspired airfoil. The primary objective of this work is to assess the efficacy of bio-inspired corrugation on the aerodynamic performance at Reynold number 80000, which can be used for modern micro aerial vehicles in the future. The goals of this study are to investigate the phenomenon responsible for the augmentation of the aerodynamic performance and static longitudinal stability of the bio-inspired corrugated airfoil and to determine the effects of corrugation on the flow structure and efficiency of the airfoil. The three CAD models of airfoils were prepared using commercial software and flow was simulated by using ANSYS Fluent software. The models were also fabricated by using a three-dimensional (3D) printing machine and aerodynamic characteristics were measured by open-ended sub-sonic wind tunnel by the varying angle of attack (AoA) from -4 to +20 degrees at a fixed Reynolds number of 80000.

2 Methodology

2.1 Airfoil Geometry

The bio-inspired corrugated airfoil cross-section derived from the mid-span section of a dragonfly wing (Aeshna cyanea) was obtained by Kesel[12] and has been named as triangular peak corrugated airfoil for this study (figure 1 a).A similar airfoil cross-section was also studied by Vergas et al.[13]. The second airfoil used in this study has been named a modified simple corrugated airfoil and was based on the airfoil given by Vargas et al.[13], however, a modification was made to this profile to match the maximum thickness of the triangular peak corrugated airfoil (figure 1 b). The third airfoil was constructed by joining the peaks of the modified simple corrugated airfoil making it a hybrid, non-corrugated airfoil, and was thus named as hybrid airfoil (figure 1 c). All three profiles (figure 1) were adjusted to have the same maximum thickness of 10.5 mm and a chord length of 80 mm. Three dimensional (3D), CAD models of all the three wings were made for these profiles for fabrication and subsequent experimentation using CATIA V5 with a span of 400 mm(Aspect ratio=5).

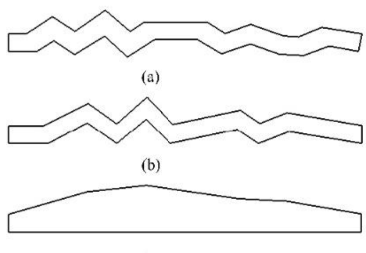

Fig. 1: Airfoil Geometries: (a) Triangular peak corrugated airfoil; (b)Modified simple corrugated airfoil; (c) Hybrid non-corrugated airfoil.

2.2 Numerical Settings

2.2.1 Computational Domain

To carry out a numerical analysis of the selected airfoils, a rectangular domain was chosen. The domain was constructed such that the domain extended for a distance 3 times the chord length (c) of the airfoil upstream of the airfoil, 5 times the chord length downstream of the airfoil, and 1.5

times the chord length above and below the airfoil (figure 2).

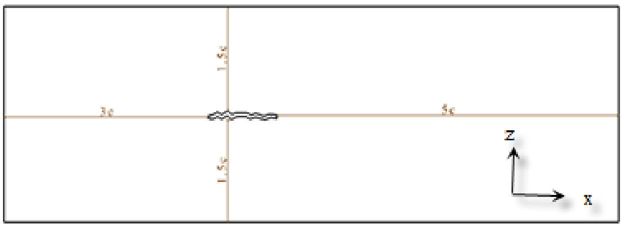

Fig. 1: Computational Domain

2.2.2 Mesh Generation

The discretization for the 2D domain has been accomplished using ANSYS software. The required element size near the airfoil surface was calculated based on the wall y+ value. To calculate the wall y+ value, the desired y value was assumed to be 11 since the Reynolds number for this study falls under the laminar flow regime. Thus, the wall spacing(Δs) value of 0.5 mm was obtained by using Eq. 1. Where y+ is a non-dimensional distance from the wall, μ is fluid kinematic viscosity, ρ is the fluid density and Ufric is the frictional velocity of the surface.

$$\Delta s = \frac{y^{+}\mu}{U_{fric}\rho} \quad (1)$$

Thus, a sphere of influence was created around the airfoil (figure 3.) with a radius of 80 mm (1.5 times the chord length of the airfoil) and an element size obtained through the wall spacing calculation as mentioned above (0.5 mm). This sphere of influence was created to improve the accuracy of the calculation by maintaining a very fine mesh within the sphere. The elements generated in the mesh are quadrilateral dominant with a face sizing of element size 1 millimeter and with an inflation of 5 layers thickness at the airfoil edges (figure 4.) which further improves the accuracy of the solution. The mesh thus generated had skewness and orthogonality with 0.35 and 0.79 respectively indicating that the mesh is of good quality (figure 5).

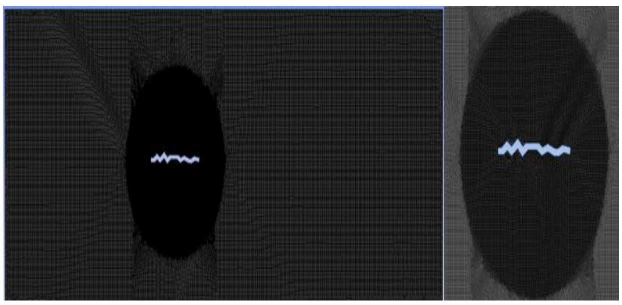
Fig. 3: Domain mesh and sphere of influence.

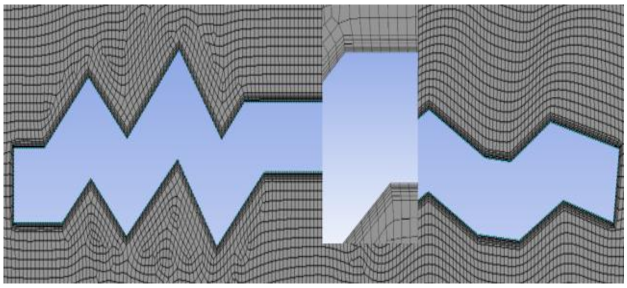
Fig. 4: Inflation around airfoil surface.

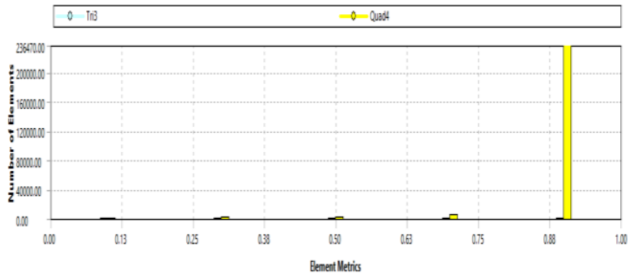

Fig. 5: Mesh Quality

2.2.3 Solver Settings

ANSYS FLUENT solver was used to conduct the CFD simulation and analysis for the airfoils. This fluent solver is based on the finite volume method. The flow Reynolds number (Re)in this study is 80,000,which falls in the laminar region and hence the flow was considered to be laminar. Since the temperature and energy changes of the flow are negligible, the energy equation is taken as constant for this simulation model.

Since the flow is incompressible as the Mach number is less than 0.3, the viscous model which is worn by K-epsilon (2-equations) with standard K-epsilon and standard wall function is been used. The solution method for velocity and pressure coupling for the SIMPLE scheme, with spatial discretization in the least square gradient with 2nd order pressure with 2nd order upwind momentum at turbulent kinetic energy and turbulent dissipation rate for both at 1st order upwind was used.

The parameter reports of lift drag and pitching moment were generated at various angles of attack from -4 to +20deg for calculation of aerodynamics performance and longitudinal stability. A residual limit of 1e-5 was set as the convergence criteria for the analysis to obtain highly accurate results.

The following equations were used to get the required parametric data from the computational analysis. The equations include RANS equation (2), equations for coefficients of lift (3), drag (4), and pitching moment (5).

$$\frac{\partial}{\partial t}(\rho u_i) + \frac{\partial}{\partial t}(\rho u_i u_j) = -\frac{\partial p}{\partial x_i} + \frac{\partial}{\partial x_j}\left[\mu\left(\frac{\partial u_i}{\partial x_j} + \frac{\partial u_j}{\partial x_i} - \frac{2}{3}\delta_{ij}\frac{\partial u_l}{\partial x_l}\right)\right] + \frac{\partial}{\partial x_j}\left(-\rho\overline{u_i' u_j'}\right) \quad (2)$$

$$C_L = \frac{L}{\frac{1}{2}\rho U_\infty^2 S} \quad (3)$$

$$C_D = \frac{D}{\frac{1}{2}\rho U_\infty^2 S} \quad (4)$$

$$C_m = \frac{M}{\frac{1}{2}\rho U_\infty^2 Sc} \quad (5)$$

In these equations the ρ is the fluid density, ui and uj are the velocity components in the x-direction, p is pressure, xi and xj are the horizontal distance, CL, CD, and CM are the coefficient of lift, drag, and pitching moment respectively, U□ is the free stream velocity, S is the area of the wing, M is pitching moment.

2.3 Experimental Setup

2.3.1 Wind Tunnel

The wind tunnel isseparated into some different parts: the convergent section, test section, and divergent section. The motor rotates the fans and the required wind velocity is developed inside the test section. Turbulence intensity is kept within the limit in the test section using honeycomb and two layers of stainless steel wire screens (figure 6). The size of the test section is 0.6x0.6x2 m. The flow velocity is measured by a 30-degree inclined tube manometer to get better accuracy. This wind tunnel can operate the free velocity ranging from 3 m/s to 50 m/s. The three forces (lift, drag, and side force) and three moments are measured by six-component balance with the help of strain gauges and the Wheat Stone bridge principle. The accuracy of velocity measurement is ± 0.5 m/s, force measurement ±0.5 N, and maximum turbulence is 1%. Six component balance is calibrated before starting the present test (figure 6). The Triangular peak corrugated airfoilis fixed inside the wind tunnel as shown in figure 7. The other wing models are also fixed similarly. There are three main sources of errors[14] during measurements of the forces and moments: accuracy of angles of attack, scale errors of the balance load cell, and errors due to variation of the density which affects the dynamic pressure (1/2 ρ V2). Considering these errors, the forces and moment evaluation were estimated to be reliable in the tested flow range.

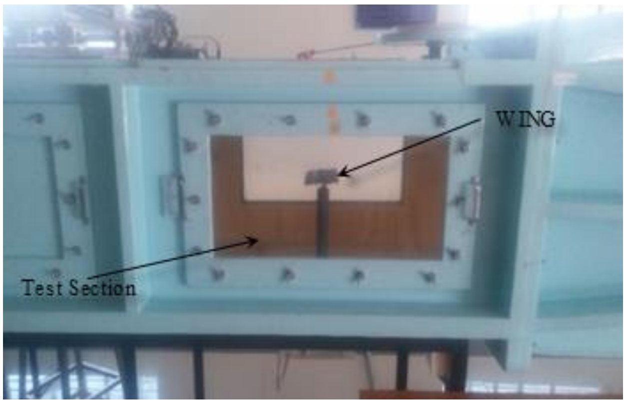

Fig. 6: A-Wing model inside the wind tunnel test section


Fig. 7: Triangular Peak Corrugated airfoil in wind tunnel test section

2.3.2 Models and Flow Condition

The first model hereafter Triangular Peak Corrugated (TPC) airfoil is obtained from the forewing of the dragonfly mid-span. The coordinates were obtained from the work of Dwivedi et al. [15]. The model is generated by putting coordinates in the CAD software. This model is the mimicking of the real forewing of the dragonfly. The thickness of the material is 4 mm, the chord is 80 mm and the span is 400 mm. The maximum thickness (tmax) is 10% of the chord (0.1c) at 40 % of the chord. This model is geometric similar to a dragonfly wing at mid-span (figure 8a).

(a)

(b)

(c)

Fig. 8: 3D printed models of (a) Triangular peak corrugated airfoil, (b) Modified simple corrugated airfoil, and (c) Hybrid airfoil.

The second model hereafter Modified Simple Corrugated (MSC) airfoil, was obtained from the work of [13]. However, the airfoil was modified by increasing the height of the second peak and also increasing the maximum thickness to match the triangular peak airfoil (figure 8b).

The third model hereafter Hybrid airfoil is a non-corrugated airfoil created by joining the peaks of the modified simple corrugated airfoil (figure 8c).

All three models have the same chord length of 80 mm and a span of 400 mm leaving a gap of 100 mm on both sides of the test section between the models and walls to avoid flow interference with the wall and wing. The height and width of the test section are 600 mm and 600 mm respectively, the blockage ratio was < 1%. A substantial gap with the wind tunnel walls is maintained to avoid the wall effects of the wind tunnel.

3 Results and Discussion

3.1 Aerodynamic Characteristics

Lift, drag, and pitching moment were the primary aerodynamic parameters calculated for the different airfoils considered over a range of 4 to 20-degree angles of attack. Plots comparing these parameters, the three airfoils were generated using MATLAB R2021a.

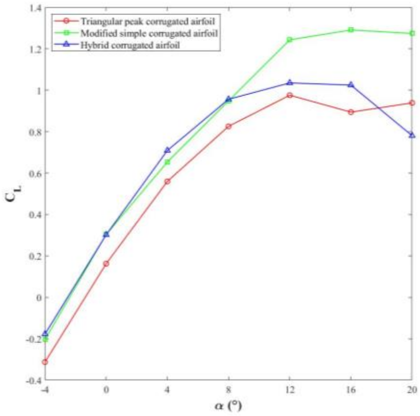

(a)

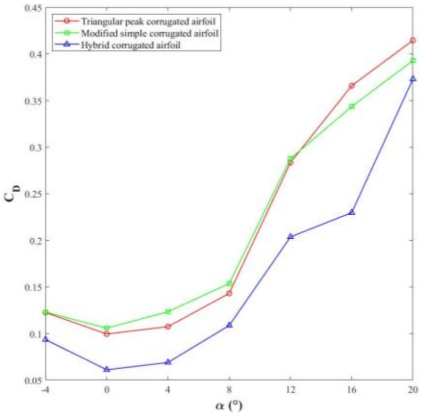

(b)

Fig. 9: (a) Variation of coefficient of lift (C_L)and b) Coefficient of drag (C_D) with the angle of attack (AOA) at Re 80000.

The plot C_L vs AOA showed that the Hybrid airfoil and the MSC airfoil were producing nearly the same amount of lift coefficient up to 8 degrees AOA, however, the TPC airfoil was producing approximately 15% lesser C_L than the other two tested airfoils. However, between 8 to 12 Degree AOA, it was observed that the rate of C_L produced by Hybrid airfoil had reduced before decreasing rapidly to 20 degrees AOA. Also, the amount of lift produced by the MSC airfoil kept on increasing significantly to 12 to 16 degrees AOA. At 20 degrees AOA, the difference in C_L between the MSC and TPC airfoil and the Hybrid airfoil was found 25%. The results alsoshowed that all the airfoils produced a negative lift at -4 degree AOA (figure. 9 a)

It is noticed from figure 9(b), that the C_D produced byboth corrugated airfoils were almost similar up to 12 degrees AOA in that the Hybrid airfoil showed the least drag coefficient. However, above 120 AOA, the C_D produced by the Hybrid airfoil increased sharply and after 160 AOA the hybrid airfoil showed the highest increase in C_D. This shows that the drag produced by Hybrid airfoils increases rapidly at high AOA whereas the corrugated airfoils show a gradual increase in C_L and a gradual decrease in C_D. Between the two corrugated airfoil profiles chosen, it was observed that the MSC airfoil consistently produced higher lift and lower drag than the TPC airfoil. Thus the MSC airfoil can provide better aerodynamic efficiency than the TPC airfoil.

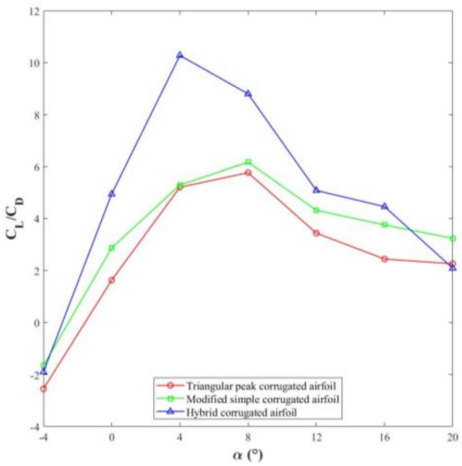

(a)

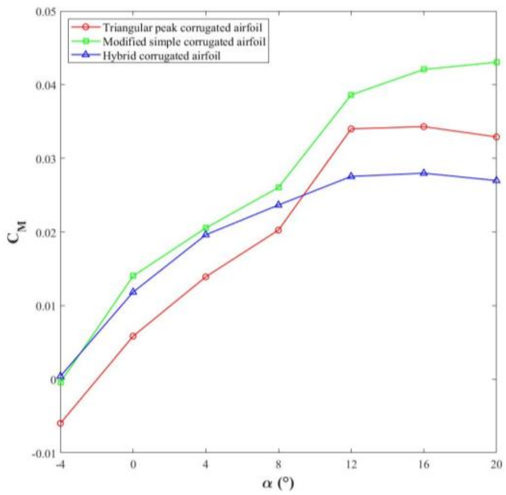

(b)

Fig. 10: (a) Variation of C_L/C_D with AOA and b) Coefficient of the moment (C_M)Vs AOA at Re 80000.

The hybrid airfoil has the highest aerodynamic performance (10) at 4 degrees AOA and then falls tremendouslyand becomes lesser than the other two tested airfoils at 20 degrees AOA and beyond. But, there is a sharp decline in the aerodynamic performance (C_L/C_D)from 10 to 2when AOA increased from 4 to 20 degrees (figure 10 a). This indicates that the Hybrid airfoil is not suitableforhigher AOA and its efficiency decreases very rapidly. However, the corrugated airfoils showed maximum aerodynamic performance of 6, at 8 degrees AOA and the decrease in performance after that wasn't as sharp as that of the Hybrid airfoil. At 20 degrees AOA, it can be seen that the Hybrid airfoil had the lowest performance among the three airfoils whereas the MSC airfoil had the best performance among all three tested airfoils. This showed that the corrugated airfoils are more efficient at higher angles of attack than conventional airfoils. Between, the two corrugated airfoils, it is clear that the MSC airfoil has better aerodynamic efficiency than the TPC across all the tested ranges of AOA up to 20 degrees. Hence, the MSC airfoil may be much more useful in flight, where there is a large variation of the angle of attack like in bio-inspired flights of insects and birds (figure 10 a).

To assess the longitudinal (pitching) static stability of the present work, the variation of the coefficient of the moment (C_M) with AOA was considered. The conditions for the longitudinal static stability are $Cm\alpha< 0$ and $Cm0> 0$. It was perceived that the pitching moment increases with an increase in AOA in all the three tested airfoils. The positive magnitude of C_M indicates the clockwise direction of the moment (nose up). Since clockwise moment increases longitudinal instability, it is desired to have a less positive C_M to ensure a stable flight. It was seen from figure 10(b) that at 40 AOA, the Hybrid airfoil and the MSC airfoil produced almost the same amount of C_M whereas the TPC airfoil produced significantly less C_M. However, as the AOA increased, the C_M produced by the corrugated airfoils increased at a higher rate than that of the Hybrid airfoil. Between 8 and 12 degrees AOA, it was observed that there is a sudden increase in the C_M produced by both the corrugated airfoils as compared to the Hybrid airfoil. Also, at 12^0 AOA, the C_M produced by the TPC airfoil exceeds that of the Hybrid airfoil. Figure 10 (b)shows that the C_M produced by both corrugated airfoils is higher than the Hybrid airfoil at high AOA. This showed that both corrugated airfoils generated high longitudinal instability at a higher angle of attack and the non-corrugated airfoil is comparatively less unstable. This instability is essential for the higher maneuverability and agility of the dragonfly as the stability and maneuverability are just the opposite of the activities.

3.2 Streamlines

Streamlines were obtained at 0-degree AOA for each profile. Figure 11(a) and 11 (b) depict the circulation of flow in the clockwise direction in the valleys of the corrugated profiles. The flow direction inside the valley is opposite to the direction of the flow in the free stream. This circulation of flow is interpreted as trapped leading-edge vortices (LEVs). These LEVs reduce the drag of the flow while providing a smoothing effect like a smooth conventional airfoil. This caused the delay in the boundary layer separation which is a phenomenon similar to that which can be observed in a golf ball as it moves through the air. This results in a reduction in the net drag produced by the corrugated airfoil. However, these trapped vortices weren't seen in the Hybrid airfoil (figure 11c) due to the absence of peaks and valleys in this configuration.

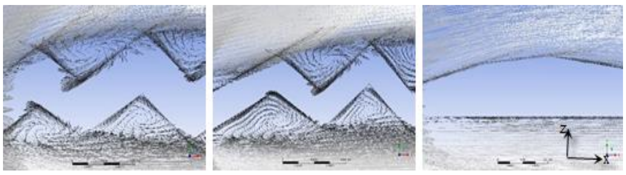

(a) (b) (c)

Fig. 11: Streamlines at 0 degrees AOA: (a) Triangular Peak airfoil; (b) Modified Simple Corrugated airfoil; (c) Hybrid airfoil.

3.3 Numerical Flow Analysis

3.3.1 Velocity Distribution

The velocity contours of the three tested airfoils are shown in figure 12. These contours are obtained by ANSYS CFD_POST for the AOA of 8, 16, and 20 degrees and Reynolds number 80,000. At 8 degrees AOA, all the corrugated airfoils showed nearly similar flow characteristics. That's why the C_L, C_D and C_L/C_D at this 8 degrees AOA for both corrugated airfoils are similar (figure 9, 10). At 16 degrees AOA, the velocity contours of the TPC airfoil had discontinuity on the upper side and the MSC airfoil was not observed. However, the Hybrid airfoil generates lesser lift and higher drag than the corrugated airfoils. Also, the flow separation was started in a Hybrid airfoil but the other two were found to be attached flow with the least drag. The high-velocity zone in TPC and MSC airfoils was found to be at 2c to 3c downstream and in Hybrid airfoils, it's less than 0.7c where c is the chord length of the airfoil. That is why a significant drop in the aerodynamic performance of the Hybrid airfoil was noticed in this AOA (Figure 10 a). This was not found in the other two airfoils. At 20 degrees AOA, the Hybrid wings velocity system is broken down and full separation with a high amount of drag was noticed.

The drag of the MSC airfoil was found 15% lesser than the triangular peaked airfoil at 20 degrees AOA. So the MSC airfoil could be used for power saving of the propulsion system. This reduction of the drag could be due to the discontinuation in velocity in the MSC airfoil and the formation of the LEVs in the corrugated airfoils.

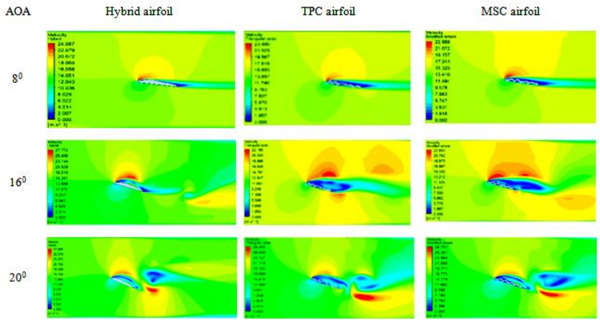

Fig. 12: Velocity contour of the Hybrid, Triangular Peak Corrugated, and Modified Simple Corrugated airfoil at Re = 80,000.

3.3.2 Pressure Distribution

The pressure contours of all the three tested airfoils are shown in figure 13 for the AOA 8, 16, and 20 degrees at Re 80,000. Up to 8 degrees AOA, the Hybrid airfoil showed better flow characteristics (high lift and less drag). However, as the AOA is increased to 16 degrees the pressure on the upper surface is reduced on the corrugated airfoils and trailing edge vortices observed in Hybrid and TPC airfoils (blue dot). This vortex was not seen in the MSC airfoil and hence the lift on the MSC airfoil is the best out of the three tested airfoils. At 20 degrees AOA, the Hybrid airfoil showed a fully chaotic flow. The corrugated airfoils showed better flow behavior than the Hybrid airfoil. The intensity of the trailing edge vortices for both corrugated wings was less than the hybrid airfoil.

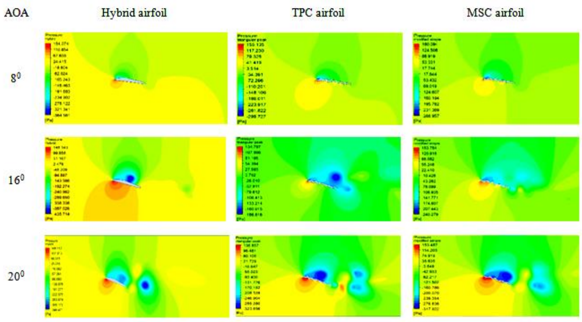

Fig. 13: Pressure distribution on the Hybrid, TPC, and MSC airfoil at Re = 80,000.

3.4 Validation

The validation of computation work was carried out by wind tunnel testing at the Institute of Aeronautical Engineering, Hyderabad, Indiaof the triangular peak airfoil as this represented the forewing of the dragonfly. Numerous research works were done in past on this airfoil and experimental results are also available to compare the present experimental and computational work. The results obtained in this study were validated by the results obtained by Murphy and Hu [6]at Re=80000. Figure 14 and figure 15 showed the comparison of the variation of the coefficient of lift and drag for AOA of the TPC airfoil for the present computational work and experimental work. The comparison showed that the results of the present computational work are less than 4% deviation up to 8 degrees AOA in the linear zone, and less than 7% deviation found up to 12 degrees AOA. The variation in results was found to be more at 16 and 20 degrees AOA. It's due to the nonlinear nature of the fluid flow behavior, which the used software might have not able to predict accurately. The experimental C_D results are very close to the computational work up to 80 AOA. However, the deviation increases more at the higher AOA. The results of the aerodynamic characteristics of the TPC airfoil match sufficiently and the results are also validated by the experimental work of Murphy and Hu [6] as shown in Figures 14 and 15.

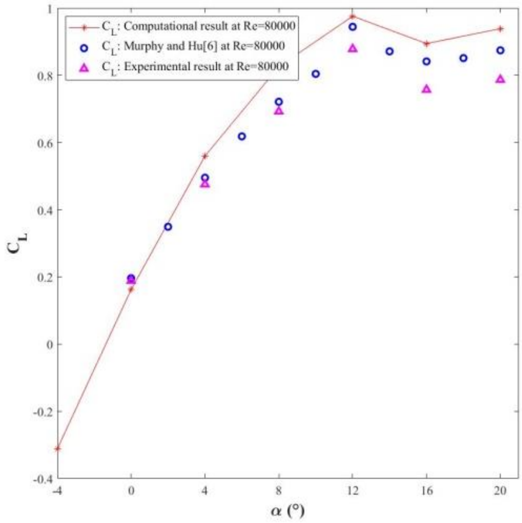

Fig. 14: Validation of results of variation of coefficient of lift (CL) with (AOA) at Re=80000.

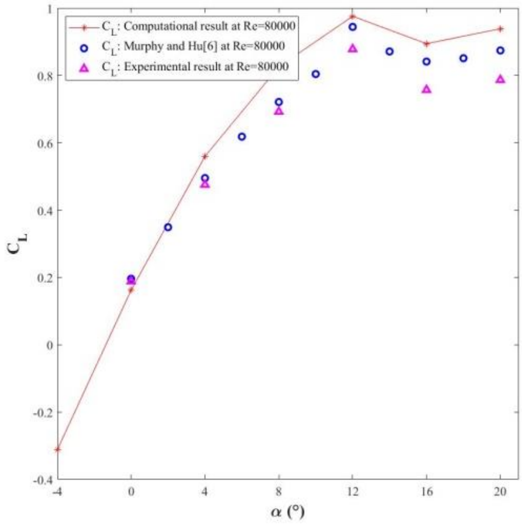

Fig. 15: Validation of results of variation of coefficient of drag (C_D) with (AOA) at Re=80000.

4 Conclusions

The following conclusions are drawn by observing the results:

- The lift coefficient (C_L) of Hybrid and modified simple corrugated (MSC) airfoils are similar up to 8 degrees AOA. However, for triangular peaked corrugated (TPC) airfoil the C_L was found 20% less than both. Above 8 degrees AOA, the MSC airfoil produced 20% more C_L in comparison with the Hybrid airfoil and 30% more than the TPC airfoil. Above 16 degrees AOA, the sharp drop of C_L of Hybrid airfoil was found to be 40%.

- The Drag coefficient (C_D) of TPC and MSC airfoils is almost similar in all tested AOA. The Hybrid airfoil showed lesser C_D among the other two airfoils ranging from 20-30% at different AOA.
- The aerodynamic performance (C_L/C_D) of the Hybrid airfoil increased to 10 at 4 degrees AOA and then falls sharply to 2 at 20 degrees AOA. The other two corrugated airfoils showed similar C_L/C_D up to 8 degrees AOA. Beyond 16 degree AOA, the MSC airfoil outperformed the remaining two airfoils.
- The longitudinal static stability of all airfoils increased with an increase in AOA up to 12 degrees and hence the $dC_M/d\alpha$ is positive. However, beyond 12 degrees AOA, the C_M of Hybrid and TPC airfoils started falling. The C_M of the MSC airfoil increased continuously up to the tested maximum AOA of 20 degrees. This showed that the Hybrid and TPC airfoils are unstable up to 12 degrees AOA. The MSC airfoil showed always unstable and no effects of AOA were felt in this airfoil.
- All these above conclusions are easily visualized by the computational simulation by noticing leading-edge vortices, pressure and velocity variations, and trapped vortices inside the valleys of the corrugation. The results are also validated by experimental work and with the existing previous work of Murphy and Hu [6].

References:

[1] K. Kawachi, "Flight Mechanism of Insect. From Standpoint of View of Bio-Fluiddynamics.," Seibutsu Butsuri, vol. 39, no. 5, Sep. (1999), DOI: 10.2142/biophys.39.279.

[2] B. Newman, S. Savage, and D. Schouella, "Model Test on a Wing Section of an Aeschna Dragonfly," Scale effects in animal locomotion, pp. 445–477, (1997).

[3] J. Wakeling and C. Ellington, "Dragonfly flight. I. Gliding flight and steady-state aerodynamic forces.," Journal of Experimental Biology, vol. 200, no. 3, pp. 543–556, Feb. (1997), DOI: 10.1242/jeb.200.3.543.

[4] C. J. C. REES, "Form and function in corrugated insect wings," Nature, vol. 256, no. 5514, pp. 200–203, Jul. (1975), DOI: 10.1038/256200a0.

[5] M. Okamoto, K. Yasuda, and A. Azuma, "Aerodynamic characteristics of the wings and body of a dragonfly," Journal of Experimental Biology, vol. 199, no. 2, pp. 281–294, Feb. (1996), DOI: 10.1242/jeb.199.2.281.

[6] J. T. Murphy and H. Hu, "An experimental study of a bio-inspired corrugated airfoil for micro air vehicle applications," Experiments in Fluids, vol. 49, no. 2, pp. 531–546, Aug. (2010), DOI: 10.1007/s00348-010-0826-z.

[7] Tsuzuki N, "A study on a miniature rotary-wing vehicle for mars exploration: its feasibility and aerodynamic characteristics of the rotor," (2005).

[8] M. Tamai, Z. Wang, G. Rajagopalan, H. Hu, and G. He, "Aerodynamic Performance of a Corrugated Dragonfly Airfoil Compared with Smooth Airfoils at Low Reynolds Numbers," (2007).

[9] A. Obata and S. Shinohara, "Flow visualization study of the aerodynamics of modeled dragonfly wings," AIAA Journal, vol. 47, no. 12, pp. 3043–3047, Dec. (2009), DOI: 10.2514/1.43836.

[10] C. J. Barnes and M. R. Visbal, "Numerical exploration of the origin of aerodynamic enhancements in [low-Reynolds number] corrugated airfoils," Physics of Fluids, vol. 25, no. 11, Aug. (2013), DOI: 10.1063/1.4832655.

[11] D. E. Levy and A. Seifert, "Simplified dragonfly airfoil aerodynamics at Reynolds numbers below 8000," Physics of Fluids, vol. 21, no. 7, (2009), DOI: 10.1063/1.3166867.

[12] A. Kesel. Aerodynamic Characteristics of Dragonfly Wing Sections Compared with Technical Airfoils. J Exp Biol; 203: 3125–3135 (2000)

[13] A. Vargas, R. Mittal, and H. Dong, "A computational study of the aerodynamic performance of a dragonfly wing section in gliding flight.," Bio inspiration & bio mimetics, vol. 3, no. 2, p. 26004, (2008), DOI: 10.1088/1748-3182/3/2/026004.

[14] É. Mangeol, D. Ishiwaki, N. Wallisky, K. Asai, and T. Nonomura, "Compressibility effects on flat-plates with serrated leading-edges at a low Reynolds number," Experiments in Fluids, vol. 58, no. 11, Nov. (2017), DOI: 10.1007/s00348-017-2443-6.

[15] Y. D. Dwivedi and Y B Sudhir Sastry, "An experimental flow field study of a bio-inspired corrugated wing at low Reynolds number," INCAS Bulletin, vol. 11, no. 3, pp. 55–65, (2019), DOI: 10.13111/2066-8201.2019.11.3.5.